ICTMS 2022 : Improved wavefront reconstruction for mask based phase-contrast tomography

Emile Barjou, Benjamin Barbrel, Francesca Mastropietro, Martin Piponnier, Benoît Recur, Aboubakr Bakkali, Pascal Desbarats

ICTMS 2022 : IMPROVED WAVEFRONT RECONSTRUCTION FOR MASK BASED PHASE-CONTRAST TOMOGRAPHY

Barjon E. [1,2]*, Badrel B. [2], Mastropietro F. [2], Pinonnier M. [4], Recur B. [3], Bakkali A. [2], Desbarats P. [1]

[1]Univ. Bordeaux, CNRS, Bordeaux INP, LaBRI, UMR 5800, F-33400 Talence, France
[2]ALPhANOV, Rue François Mitterrand, 33400, Talence, France
[3]INSERM LAMC U1029, Allée Geoffroy Saint Hilaire, 33615 Pessac Cedex, France
[4]Imagine Optics, Rue François Mitterrand, 33400, Talence, France

INTRODUCTION

Phase-contrast imaging (PCI) is a promising technique that became practical in laboratory setups thanks to high-power microfocus X-Ray sources [1]. Coupled with high-resolution (HR) detectors, HR-PCI can be achieved in a single exposure using Hartmann masks, which captures the sample-induced deformation of the x-ray wavefront (WF) through the local deflections of X-rays. The reconstructed wavefront then provides information on the complex index of refraction of the sample [2,3].
With accurate measurement of the projected phase shifts, a phase tomogram can be reconstructed to obtain localized information on the sample material.

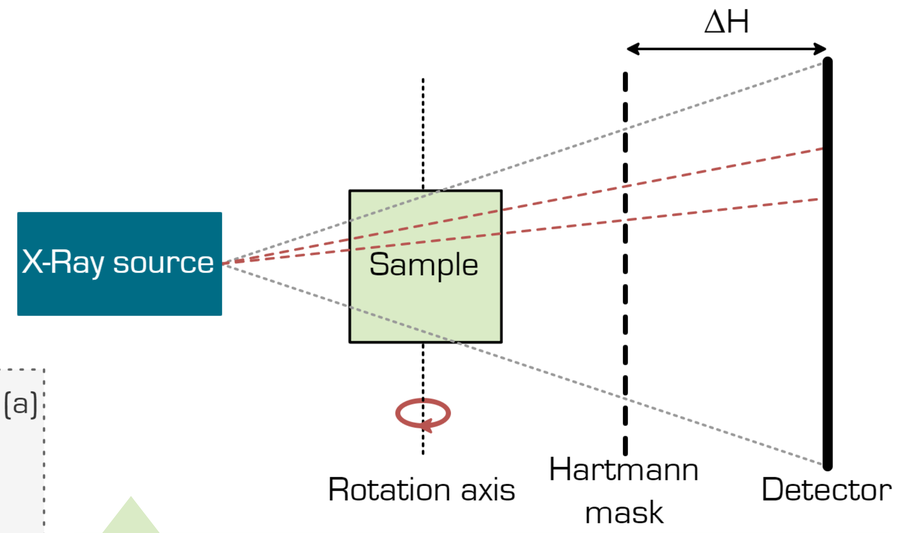

Fig. 1 : Diagram of our acquisition setup.

WAVEFRONT RECONSTRUCTION

Algorithms dedicated to reconstruct wavefront (WF) acquired using Hartmann sensors have been largely described in literature. The most common is described in [4] as an iterative reconstruction algorithm (IR-WF).

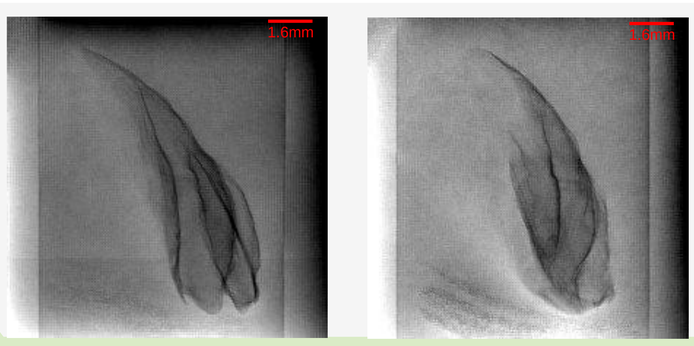

Fig. 3: Examples of direct WF reconstruction of a juvenile oyster shell at different angles.
By processing each projection individually, artifacts appear due to the noise in the deflection maps. Those incoherent artifacts alter the tomographic reconstruction.

TOMOGRAPHY + IR-WF

To improve the homogeneity between the projections during IR-WF, we developed a 3D-driven algorithm that converges on the volume rather than the projections. An IR-WF iteration is applied to the current volume projection, and then compared to the raw projection to compute the error to back-propagate.

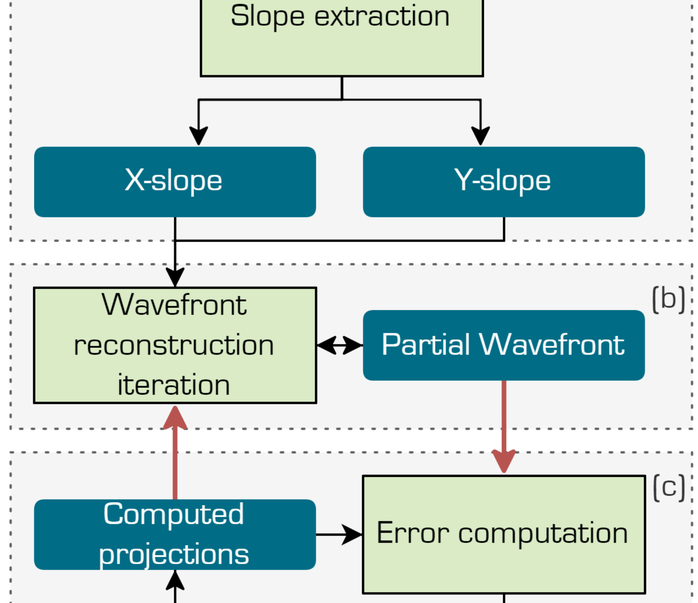

Fig. 4 : Diagram of the simultaneous WF and CT reconstructions. Both reconstructions converge simultaneously, ensuring that any single wavefront has to be coherent with all others.

HARTMANN SENSOR

A Hartmann sensor consists of a mask drilled with a micrometric holes placed in front of a detector, that defines an array of beamlets.
The phase-related information is contained in the deflection of the individual beamlets. Different Hartmann configurations were tested in our setup to improve deflection sensitivity, spatial resolution and SNR.

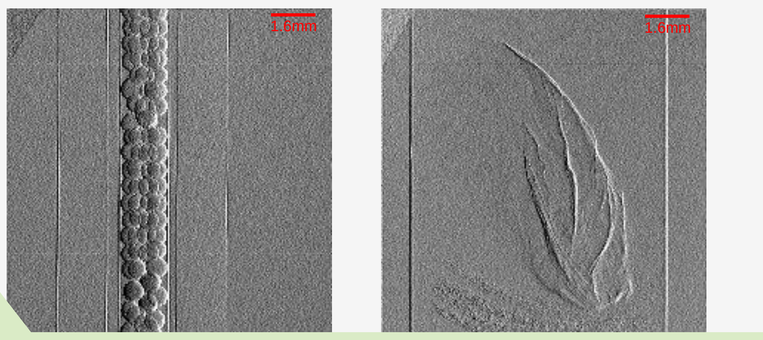

Fig. 2 : Examples of horizontal deflections extracted from the raw image acquired with this setup on two samples. (a) Shell of a juvenile oyster from Institut Fresnel, Marseille. (b) Tube filled with glass silicate microspheres.

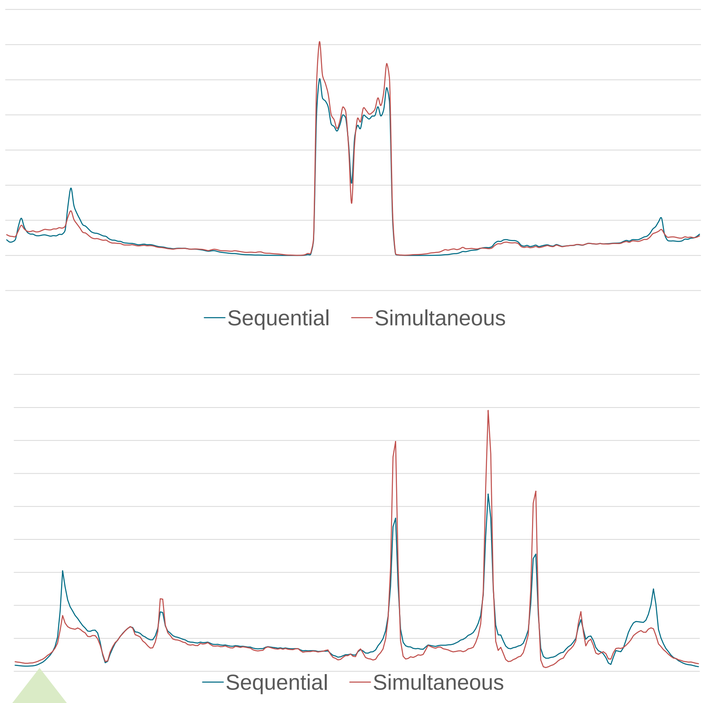

Plot. 1 : Gray level along the lines of the example layers, for both sequential and simultaneous reconstructions.

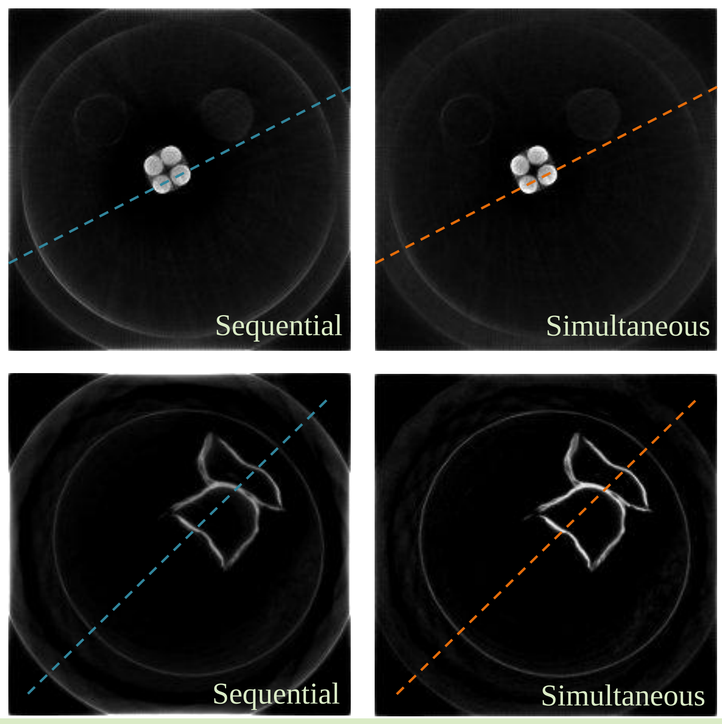

	Sequential	Simultaneous
PSNR local	11,016	12,107
PSNR full	11,685	15,519
SNR local	0,634	1,279
SNR full	0,863	0,924
CNR local	11,016	27,062
CNR full	10,088	14,333

	Sequential	Simultaneous
PSNR local	6,265	9,643
PSNR full	9,242	9,406
SNR local	1,055	2,315
SNR full	1,075	1,259
CNR local	6,100	19,128
CNR full	9,916	11,789

Tab. 1 : Metrics measured from the example layers.
Local metrics are obtained by manually selecting the signal and noise regions of interest, while the full metrics are obtained on the complete image without segmentation.

Formula used :
SNR = Mean/StdDev
PSNR = Max/StdDev
CNR = (Max-Min)/StdDev

RESULTS COMPARISON

This method allows to retrieve a more homogeneous result with both better contrast-to-noise and signal-to-noise ratios than the consecutive application of IR-WF and IR-CT in both sample datasets.
Since only the order of the operations differs, the computation time for the two methods is similar.

References:
[1] Alberto Bravin, et al. "X-ray phase-contrast imaging: from pre-clinical applications towards clinics.". Physics in medicine and biology 58 1. (2013): R1-35 .
[2] Begani Provinciali, Ginevra et al. "High-Sensitivity X-ray Phase Imaging System Based on a Hartmann Wavefront Sensor". Condensed Matter 7. (2021).
[3] La Rochefoucauld, Ombeline et al. "EUV and Hard X-ray Hartmann Wavefront Sensing for Optical Metrology, Alignment and Phase Imaging". Sensors 21. 3(2021).
[4] W.H. Southwell, . "Wave-front estimation from wave-front slope measurements". J. Opt. Soc. Am. 70. 8(1980): 998–1006.

Acknowledgements: this study was done within the context of the XPulse project, funded by the Nouvelle-Aquitaine region and the ERDF.

ALPhANOV - Optics and Lasers Technology Center
Institut d'Optique d'Aquitaine - Rue François Mitterrand
33400 - France - Ph.: +33 (0)5 54 24 52 00
info@alphanov.com - www.alphanov.com